important to prevent outbreaks of *Mycoplasma* mastitis on dairy farms. It has been reported that *M bovis* could be detected in bulk tank milk on a farm where only one out of 300 cows was excreting organisms (Bicknell and others 1983). In the present study, it was confirmed that 1.8 (farm 12; 3/166) to 6.1 per cent (farm 13; 11/180) of *M bovis*-infected cows and 6.9 (farm 14, 18/258) to 8.3 per cent (farm 3, 5/60) of *M californicum*-infected cows on dairy farms were sufficient to detect *Mycoplasma* mastitis by bulk tank milk screening.

References

ARCANGIOLI, M. A., CHAZEL, M., SELLAL, E., BOTREL, M. A., BEZILLE, P., POUMARAT, F., CALAVAS, D. & LE GRAND, D. (2011) Prevalence of *Mycoplasma bovis* udder infection in dairy cattle: preliminary field investigation in southeast France. *New Zealand Veterinary Journal* **59,** 75-78

BICKNELL, S. R., GUNNING, R. F., JACKSON, G., BOUGHTON, E. & WILSON, C. D. (1983) Eradication of *Mycoplasma bovis* infection from a dairy herd in Great Britain. *Veterinary Record* **112,** 294-297

HALE, H. H., HELMBOLDT, C. F., PLASTRIDGE, W. N. & STULA, E. F. (1962) Bovine mastitis caused by a *Mycoplasma* species. *Cornell Veterinarian* **52,** 582-591

HIGUCHI, H., IWANO, H., KAWAI, K., OHTA, T., OBAYASHI, T., HIROSE, K., ITO, N., YOKOTA, H., TAMURA, Y. & NAGAHATA, H. (2011) A simplified PCR assay for fast and easy *Mycoplasma* mastitis screening in dairy cattle. *Journal of Veterinary Science* **12,** 191-193

JASPER, D. E., DELLINGER, J. D., ROLLINS, M. H. & HAKANSON, H. D. (1979) Prevalence of mycoplasmal bovine mastitis in California. *American Journal of Veterinary Research* **40,** 1043-1047

JELINEK, P. D., DEVEREAUX, D. J., MARTIN, P. A. & BULLER, N. B. (1993) A survey for *Mycoplasmas* in bulk-tank milk of dairy herds in Western Australia. *Australian Veterinary Journal* **70,** 30

KIRK, J. H., GLENN, K., RUIZ, L. & SMITH, E. (1997) Epidemiologic analysis of *Mycoplasma* species isolated from bulk-tank milk samples obtained from dairy herds that were members of a milk cooperative. *Journal of the American Veterinary Medical Association* **211,** 1036-1038

MCDONALD, W. L., RAWDON, T. G., FITZMAURICE, J., BOLOTOVSKI, I., VOGES, H., HUMPHREY, S., FERNANDO, K., CANAGASEBEY, Y., THORNTON, R. N. & MCINTYRE, L. (2009) Survey of bulk tank milk in New Zealand for *Mycoplasma bovis*, using species-specific nested PCR and culture. *New Zealand Veterinary Journal* **57,** 44-49

NICHOLAS, R. A. & AYLING, R. D. (2003) *Mycoplasma bovis*: disease, diagnosis, and control. *Research in Veterinary Science* **74,** 105-112

PASSCHYN, P., PIEPERS, S., DE MEULEMEESTER, L., BOYEN, F., HAESEBROUCK, F. & DE VLIEGHER, S. (2011) Between-herd prevalence of *Mycoplasma bovis* in bulk milk in Flanders, Belgium. *Research in Veterinary Science.* In Press

Prevalence of *Mycoplasma* species in bulk tank milk in Japan

H. Higuchi, H. Iwano, S. Gondaira, et al.

Veterinary Record 2011 169: 442 originally published online September 15, 2011
doi: 10.1136/vr.d5331

Biol Trace Elem Res (2012) 145:166–171
DOI 10.1007/s12011-011-9180-0

Analysis of Trace and Major Elements in Bronchoalveolar Lavage Fluid of Mycoplasma Bronchopneumonia in Calves

Kazuyuki Suzuki · Hidetoshi Higuchi · Hidetomo Iwano · Jeffrey Lakritz · Kouichiro Sera · Masateru Koiwa · Kiyoshi Taguchi

Received: 30 May 2011 / Accepted: 12 August 2011 / Published online: 26 August 2011

Abstract The aim of this study was to evaluate the reliability and effectiveness of direct determination of trace and major element concentrations in bronchoalveolar lavage fluid samples from Holstein calves with *Mycoplasma* bronchopneumonia (n=21) and healthy controls (n=20). The samples were obtained during bronchoscopy using a standard examination method. A total of 18 elements (aluminum, bromine, calcium, chlorine, chromium, copper, iron, potassium, magnesium, manganese, molybdenum, nickel, phosphorous, sulfur, silicon, strontium, titanium, and zinc) were detected by particle-induced X-ray emission. The average bromine, iron, potassium, magnesium, and phosphorous concentrations were higher in calves with bronchopneumonia than in controls ($p<0.05$). They were found to have higher amounts of calcium and zinc, and a higher zinc–copper ratio than that in healthy calves ($p<0.001$). Based on the receiver operating characteristics curves, we propose a diagnostic cutoff point for zinc–copper ratio for identification of *Mycoplasma* pneumonia of 8.676. Our results indicate that assessment of the elemental composition of broncholaveolar lavage fluid is a promising diagnostic tool for *Mycoplasma* bronchopneumonia.

Keywords Bronchoalveolar lavage fluid · Calf · Trace elements · *Mycoplasma* bronchopneumonia · PIXE

Abbreviations

BALF	Bronchoalveolar lavage fluid
MMP	Matrix metalloproteinase
PCR	Polymerase chain reaction
PIMs	Pulmonary intravascular macrophages
PIXE	Particle-induced X-ray emission
ROC	Receiver operating characteristic

Introduction

Mycoplasma bovis is an important cause of calf pneumonia worldwide. Because immune prophylaxis and treatment with antibiotics are not very effective, control measures must include the introduction of strict hygiene standards, confinement of infected herds, and culling of clinically diseased animals [1]. Infection by *M. bovis* may develop into a severe suppurative bronchopneumonia or necrotizing pneumonia when associated with other organisms or, conversely, into a mild catarrhal broncho-interstitial pneumonia when associated with other microorganisms [2]. Pulmonary lesions in naturally infected calves comprise an exudative bronchopneumonia and extensive foci of coagulative necrosis surrounded by inflammatory cells [2]. Chronic infections are often associated with a lymphocytic "cuffing" pneumonia with marked hyperplasia of peribronchial lymphoid tissue that causes stenosis of the airway lumen and compression and collapse of adjacent pulmonary parenchyma [1].

K. Suzuki (✉) · H. Higuchi · H. Iwano · M. Koiwa · K. Taguchi
School of Veterinary Medicine, Rakuno Gakuen University,
582 Midorimati, Bunnkyoudai,
Ebetsu, Hokkaido 069-8501, Japan
e-mail: kazuyuki@rakuno.ac.jp

K. Suzuki · J. Lakritz
College of Veterinary Medical Science, Ohio State University,
601 Vernon L. Tharp St.,
Columbus, OH 43210-1089, USA

K. Sera
Cyclotron Research Center, Iwate Medical University,
Tomegamori,
Takizawa, Iwate 020-0173, Japan

Pulmonary intravascular macrophages (PIMs) are present in ruminants and horses [3]. These species are highly sensitive to acute lung inflammation compared with non-PIM-containing species such as rats and humans. As the source of TNF-alpha, PIMs promote recruitment of inflammatory cells including IL-8-containing platelets to stimulate acute inflammation in lungs [3]. Lung injury in human and animals are associated with modifications of the extracellular matrix metabolism that lead to an accumulation of several elements and the development of organ fibrosis [3]. In inflamed lungs, matrix metalloproteinase (MMP)-9 is a key contributor to degradation of lung tissue and it potentiates activation of neutrophil chemotactic chemokines. MMP-9 is overexpressed in inflammatory pulmonary disorders of lung in human with adult respiratory distress syndrome [4]. Elevated levels of both serine proteinases and MMPs have been reported in bronchoalveolar lavage fluid (BALF) taken from humans with adult respiratory distress syndrome [4, 5], dogs with pulmonary eosinophilia [6] and horses with chronic obstructive pulmonary disease [7]. Lakritz et al. [8] indicated that gelatinases MMP-2 and MMP-9 were detected in BALF of healthy calves and that lipopolysaccharide-stimulated alveolar macrophages express MMP-9. In addition, an association between pneumonias attributable to *Pasteurella multocida* or *Mycoplasma bovirhinis* in calves and accumulation of MMP-9 in tracheobronchial lavage fluid has been reported [9]. MMPs are a family of zinc and calcium-dependent endopeptidases involved in remodeling and physiological homeostasis of extracellular matrix [10]. Therefore, it is important to investigate the relevance of bronchopneumonia and trace and major element status for food animal health care. However, no comparative studies are available on the trace and major elements status in BALF form calves with *Mycoplasma* bronchopneumonia.

Thus, the aim of this study was to investigate the concentrations and relationships between trace and major elements in BALF from calves with *Mycoplasma* bronchopneumonia. The receivers operating characteristic (ROC) curves were used to describe the performance of BALF in screening for *Mycoplasma* bronchopneumonia and to propose diagnostic cutoffs for calves.

Materials and Methods

All procedures were performed in accordance with the Guide for the Care and Use of Laboratory Animals of the School of Veterinary Medicine at Rakuno Gakuen University and the National Research Council [11].

Forty-one Holstein calves, 31 males and 10 females, aged 85.3±46.1 days old, were enrolled in this study. The health status of the animals was established on the basis of physical, biochemical, thoracic ultrasound, and radiological examinations. Twenty-one calves were isolated at the Rakuno Gakuen University Veterinary Teaching Hospital showing clinical signs such as coughing, nasal discharge, fever, and pulmonary wheezing sounds. As controls, 20 healthy calves with none of these clinical symptoms were kept at the School of Veterinary Medicine, Rakuno Gakuen University.

The BALF samples were obtained during bronchoscopic examination using a standard protocol described elsewhere [12–14]. Briefly, bronchoscopy was performed using a flexible video bronchoscope (Olympus VQ Type 6092A, Olympus Co., Tokyo, Japan) under sedation with 0.05 mg/kg of 2% xylazine solution. The tip of the bronchoscope was wedged into a position in a tracheal bronchus. Two hundred milliliters isotonic, sterile saline solution warmed to 37°C was instilled in 50 mL portions with a disposable plastic syringe and immediately re-aspirated. The first aliquot was discarded [14]. In this procedure, a recovery rate of at least 60% is required.

Sub-samples were cultivated and investigated by polymerase chain reaction (PCR) tests targeting the *M. bovis*, based on 16S rRNA genes [15]. Briefly, simplified PCR was performed in a total reaction volume of 20 μL containing 10 μL of 2× AmpdirectPlus (Shimadzu Co., Kyoto, Japan), 0.5 U of Nova taq TM Hot Start DNA polymerase (Novagen, UK), 5 pmol of a mycoplasma universal primer set (MycoAce; Nihon Dobutsu Tokusyu Shindan Ltd., Hokkaido, Japan), and 5 μL of each samples. PCR was performed in an iCycler PCR System (Bio-Rad Laboratories, USA). Conditions for the simplified PCR were as follows: initial denaturation at 95°C for 10 min followed by 35 cycles of denaturation at 94°C for 30 s, annealing at 60°C for 45 s, and extension at 72°C for 1 min. The PCR products were separated by electrophoresis on 1.5% (*w/v*) agarose gels, stained with ethidium bromide, and visualized with a UV trans-illuminator. The *M. bovis* strain (ATCC 25523) was used as positive standard.

The BALF was then centrifuged at 180×*g* for 10 min at 4°C to remove cell debris and the supernatant was stored at −80°C until assay. The mean concentrations of trace and major elements in BALF were detected by the particle-induced X-ray emission (PIXE) method. A detailed description of the experimental arrangement is shown elsewhere [13, 16]. Briefly, 100 μL BALF supernatants were placed on a subtlety Myler membrane and desiccated. The supernatants were directly irradiated with proton beams. A small (baby) cyclotron used for positron nuclear medicine at the Nishina Memorial Cyclotron Center (Iwate, Japan) provides a 2.9-MeV proton beam on a target after passing through a graphite beam collimator. A Si (Li) detector (0.0254 mm Be window) with 300 and 1,000-μm thick Mylar absorbers was used to select X-rays with energy higher than that of K–K alpha. For lower-energy X-rays, another Si (Li) detector (0.008 mm Be) was used without absorber.

The data are shown as means±standard deviation (SD). Statistical analyses were performed using a commercial software package from IBM SPSS Statistics, v.19 (IBM Co, Somers, NY, USA). The mean values for each dependent variable were compared to the control values using the unpaired Student's t test after analysis of ANOVA as F test. The ROC curves were used to characterize the sensitivity and specificity of a parameter to *Mycoplasma* bronchopneumonia. The optimal cutoff point for a test was calculated by the Youden index [17]. The Youden index (J) is defined as the maximum vertical distance between the ROC curve and the diagonal or chance line and is calculated as J=maximum [sensitivity+specificity−1]. The cutoff point on the ROC curves that corresponds to J is taken to be the optimal cutoff point [17]. The significance level was set at $p<0.05$.

Results

Figure 1 shows the detection of *M. bovis* by simplified PCR based on 16S rRNA genes. The PCR for *Mollicutes* detected *M. bovis* in only one sample (5%) from a healthy calves (controls, n=20) and in all samples (n=21, 100%) from calves with bronchopneumonia. Therefore, the statistical analysis enrolled 19 healthy controls that had not detected *M. bovis* and 21 bronchopneumonia calves.

The mean concentrations of trace and major elements in BALF from calves with *Mycoplasma* bronchopneumonia are summarized in Table 1. The PIXE method allowed detection of 18 elements: Al, Br, Ca, Cl, Cr, Cu, Fe, K, Mg, Mn, Mo, Ni, P, S, Si, Sr, Ti, and Zn. The average concentrations of Br, Fe, K, Mg, and P were higher in the calves with bronchopneumonia than those of the controls ($p<0.05$). Additionally, the calves with *Mycoplasma* bronchopneumonia were found to have larger amounts of Ca and Zn compared to those without respiratory disease ($p<0.01$ and $p<0.001$, respectively). There are no significant differences in the levels of the remaining 11 elements.

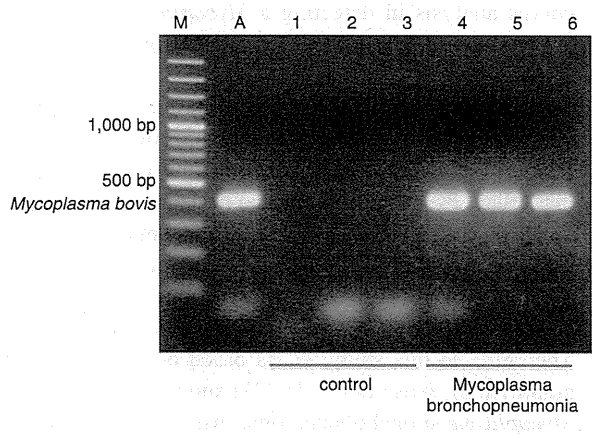

Fig. 1 Detection of *Mycoplasma bovis* in calves by polymerase chain reaction based on 16S rRNA genes. *M* marker, *A* positive standard (ATCC 25523), *lanes 1–3* control, and *lanes 4–6* bronchopneumonia calves

Table 1 Comparison of 18 trace and major elements status measured in broncoalveolar lavage fluid of the calves with or without *Mycoplasma* bronchopneumonia

(μg/mL)	Control (n=19)	*Mycoplasma* pnuemonia (n=21)	p value
Al	0.365[a]±0.238	0.942±0.924	NS[b]
Br	0.409±0.203	1.010±0.814	$p<0.05$
Ca	4.78±1.62	10.05±6.92	$p<0.01$
Cl	704.3±176.4	1,110.4±874.0	NS
Cr	0.028±0.016	0.038±0.021	NS
Cu	0.026±0.036	0.034±0.040	NS
Fe	0.099±0.070	0.201±0.190	$p<0.05$
K	34.4±12.5	65.3±32.9	$p<0.05$
Mg	1.13±0.75	3.11±2.39	$p<0.05$
Mn	0.012±0.008	0.014±0.016	NS
Mo	0.052±0.036	0.029±0.025	NS
Ni	0.009±0.005	0.007±0.005	NS
P	3.21±1.89	15.33±10.45	$p<0.05$
S	8.62±2.26	27.35±21.23	NS
Si	1.19±0.68	1.93±1.09	NS
Sr	0.017±0.015	0.016±0.016	NS
Ti	0.094±0.085	0.124±0.058	NS
Zn	0.074±0.048	0.366±0.166	$p<0.001$
Ca/P	2.01±1.63	1.01±0.66	NS
Zn/Cu	5.93±5.48	26.84±19.57	$p<0.001$

[a] micrograms per liter (μg/mL)

[b] Not significant

The areas under the ROC curves for Ca and Zn concentrations were 0.779 ($p<0.01$) and 0.990 ($p<0.001$), respectively (Fig. 2). The proposed diagnostic cutoff points for Ca and Zn concentrations in BALF for identifying *Mycoplasma* bronchopneumonia based on the analysis of the ROC curves were set at 5.894 and 0.180 μg/mL, respectively. Sensitivities and specificities of proposed diagnostic cutoffs for Ca concentration in BALF were 71.4% and 90.0%, respectively. In the same manner, sensitivities and specificities of proposed diagnostic cutoffs for Zn concentration in BALF were 95.2% and 95.0%, respectively.

Figure 3 shows a ROC curves for Zn/Cu ration in detecting *Mycoplasma* bronchopneumonia in calves. In the body, Ca and P, and Zn and Cu are regulated and restricted by each other, so variations in the Ca/P and the Zn/Cu ratios reflect the effects of these two microelements, respectively [13, 16]. However, in the calves with *Mycoplasma* bronchopneumonia, no characteristic difference of the Ca/P ratio was found in BALF. In contrast, the Zn/Cu ratios of

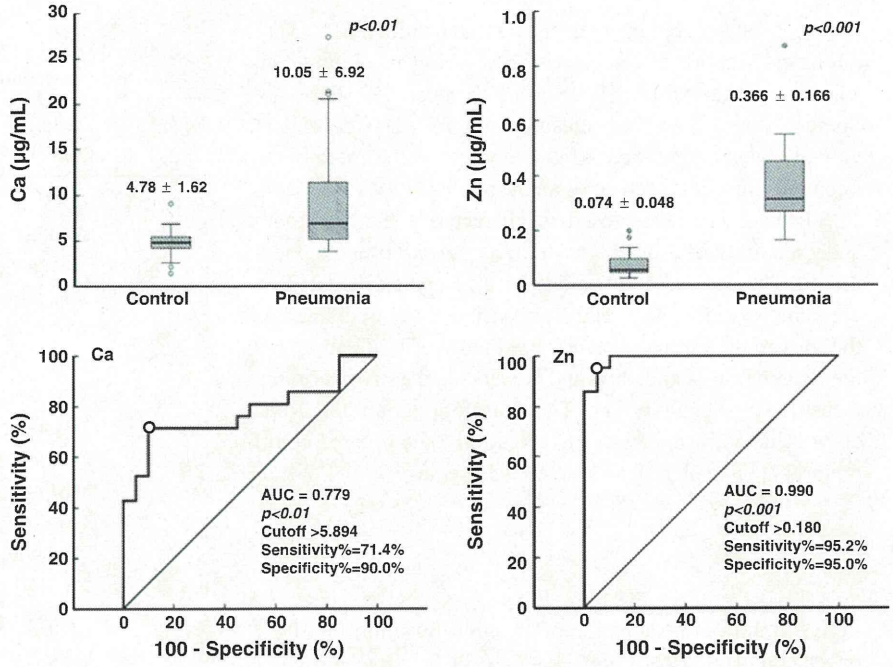

Fig. 2 Receiver operating characteristic (ROC) curves for Ca and Zn concentrations for detection of *Mycoplasma* bronchopneumonia in calves. The mean area under the ROC curve (AUC) is shown for each ROC curve. The optimal cutoff point for test was calculated by the Youden index. *Open circle* cutoff point

the BALF in the calves with *Mycoplasma* bronchopneumonia (26.84±19.57) were significantly higher than that of the healthy control (4.91±3.48, $p<0.001$). Proposed diagnostic cutoff points for Zn/Cu ratios in BALF for identifying *Mycoplasma* pneumonia based on the analysis of the ROC curves were set at 8.676. Sensitivities and specificities of proposed diagnostic cutoffs for Zn/Cu ratio in BALF were 93.8% and 82.4%, respectively.

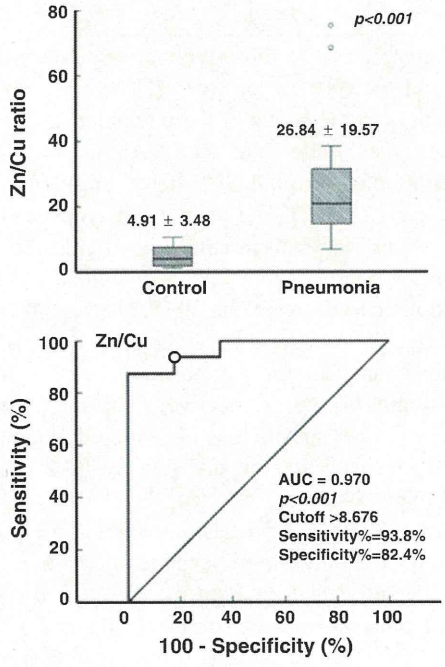

Fig. 3 Receiver operating characteristic (ROC) curves for the Zn/Cu ratio for detection of *Mycoplasma* bronchopneumonia in calves. See Fig. 2 for key

Discussion

We found how *Mycoplasma* bronchopneumonia in calves is associated with the concentrations of some trace and major elements in BALF. The calves with *Mycoplasma* bronchopneumonia were found to have larger concentrations of Br, Ca, Fe, K, Mg, P and Zn, and a high Zn/Cu ratio in BALF compared to those without bronchopneumonia. In addition, the proposed diagnostic cutoffs for Ca and Zn concentrations and Zn/Cu ratio in BALF based on ROC curves analysis in detecting a *Mycoplasma* bronchopneumonia were set at 5.894 and 0.180 μg/mL, and 8.676, respectively.

The clinical and pathological signs for bronchopneumonia caused by *M. bovis* are non-specific, so laboratory diagnosis is necessary for identification of the disease. To that effect, PCRs have been used to detect *M. bovis* directly in milk and nasal samples [18]. Several researches demonstrated that sampling by BALF was more useful for prediction of lower respiratory airway pathogens than nasal swabs although clearly not as convenient [19, 20]. Therefore, in this study, PCRs based on 16S rRNA genes amplified *M. bovis* DNA [15, 21] and were used to confirm *Mycoplasma* bronchopneumonia, using BALF samples.

The PIXE method used in the present study is a fast and reliable multi-element qualitative and quantitative analytical tool that is easily accomplished [22]. In this technique, a

detector analyzes characteristic X-rays emitted as a result of inner-shell ionization of target atoms. The method works well in small samples and is suitable for determining elements in a solid surface, especially for analyzing medium and higher atomic weight elements in a matrix consisting of light elements. With this technique, a sample of a few micrograms is sufficient to analyze concentrations in the parts-per-million range [22]. Because the method does not involve complicated sample preparation, the risk of contamination during the preparation of a sample for PIXE method is remarkably lower than that for other methods [13, 16].

Our results show that the average Br, Fe, K, Mg, and P concentrations in BALF from bronchopneumonia calves were higher than those in controls. A structurally and functionally distinct enzyme from neutrophil myeloperoxidase has the unique ability to use halides or pseudohalides (X^-) and H_2O_2 derived from the respiratory burst to generate cytotoxic hypohalous acids, especially hypobromous acid (HOBr) [23, 24]. The eosinophil peroxidase (EPO), such as EPO–H_2O_2–Br^- system, is also an effective cytotoxin for multiple targets such as multicellular worms or parasites, bacteria, viruses, and host cells [23]. Both HOBr and the EPO–H_2O_2–Br^- system are involved in many of the pathophysiological features of inflamed respiratory disease [24].

Iron is involved in many enzymatic activities. Significant changes in Fe concentration have been reported in BALF of patients with acute respiratory distress syndrome [25]. These changes have been interpreted as indicating that lungs require basal levels of extracellular redox-active Fe [26].

Potassium, magnesium, and phosphorus leak out to the extracellular fluid from tracheal epithelial cell injury because these elements are mostly contained in the intracellular fluid. Majeschak et al. [27] suggested that the Mg^{2+}/ATP-dependent 26S proteasome complex exists outside the cell and is released into the lung epithelial lining fluid after lung injury and contributes to the proteolysis of the bulk of protein in the alveolar space. BAL phospholipid content in lung injury rats correlated with the severity of alveolar-capillary leak [3]. Therefore, increased levels of Br, K, Fe, Mg, and P in BAL might be highly correlated with bronchial inflammation caused by *M. bovis*.

It was also found that BALF from calves with *Mycoplasma* bronchopneumonia were found to have larger concentrations of Ca and Zn and a high Zn/Cu ratio compared to those without respiratory disease. It is known that a calcium ionophore induces airway hyper-responsiveness to intravenous histamine and substance P possibly by reducing the nitric oxide levels in the airway tissues. This may be due to damaged airway epithelium and/or NO breakdown by activated inflammatory cells in the airway [28]. It is speculated that there is a correlation between Ca levels in BALF and the damage of the airway epithelium in calves with *Mycoplasma* bronchopneumonia. MMPs are a family of Zn and Ca-dependent endopeptidases involved in remodeling and physiological homeostasis of the extracellular matrix, shown to be important in the early stages of inflammation associated with respiratory disease in cattle [8, 29].

Associations between pneumonias attributable to *P. multocida* or *M. bovirhinis* in calves and accumulation of MMP-9 in tracheobronchial lavage fluid have been reported [9]. These molecules have high Zn-binding ability, containing three Zn-binding histidines and a glutamate that acts as a general base/acid during catalysis [30]. Furthermore, MMPs have three α-helices and a five-stranded β-sheet, as well as at least two Ca sites and a second Zn site with structural functions. Consequently, MMPs depend upon ionized Zn for activity and on Ca for stability. The changes of these elements are not specific with *Mycoplasma* bronchopneumonia because they result from reactions to inflammation of the bronchus and the tracheal branches. However, *Mycoplasma* bronchopneumonia induces severe airway inflammation accompanied by profound and persistent micro-vascular remodeling in tracheobronchial mucosa. The present results support these findings.

The pathogenesis of *Mycoplasma* bronchopneumonia is usually studied by genetic, proteomic, or molecular biology approaches. This study suggests that direct determination of trace and major elements concentrations in BALF could be a useful approach to the study of the pathogenesis of *Mycoplasma* bronchopneumonia. Infected calves were found to have higher amounts of Ca and Zn and a high Zn/Cu ratio in BALF compared to those without respiratory disease.

In conclusion, it is suggested that measuring the Br, Ca, Fe, K, Mg, P, and Zn concentrations and the Zn/Cu ratio status in BALF might help with diagnosis and even predict the susceptibility of a calf to *Mycoplasma* bronchoneumonia. Future studies need to focus in determining whether there is a correlation between zinc and calcium levels in BALF and the severity of bronchopneumonia.

Acknowledgments This study was supported by a grant-in-aid for Science Research from the Ministry of Education, Culture and Sciences of Japan (no.21580393) awarded to K. Suzuki and by a grant from Rakuno Gakuen University Research to K. Suzuki.

References

1. Nicholas RA, Ayling RD, McAuliffe L (2009) Vaccines for *Mycoplasma* diseases in animals and man. J Comp Pathol 140 (2–3):85–96
2. Radaelli E, Luini M, Loria GR et al (2008) Bacteriological, serological, pathological and immunohistochemical studies of *Mycoplasma bovis* respiratory infection in veal calves and adult cattle at slaughter. Res Vet Sci 85(2):282–290
3. Singh B, Pearce JW, Gamage LN et al (2004) Depletion of pulmonary intravascular macrophages inhibits acute lung inflammation. Am J Physiol Lung Cell Mol Physiol 286(2):L363–L372

4. Parks WC, Shapiro SD (2001) Matrix metalloproteinases in lung biology. Respir Res 2:10–19
5. Torii K, Iida K, Miyazaki Y et al (1997) Higher concentrations of matrix metalloproteinases in bronchoalveolar lavage fluid of patients with adult respiratory distress syndrome. Am J Respir Crit Care Med 155:43–46
6. Rajamäki MM, Järvinen AK, Sorsa T et al (2002) Clinical findings, bronchoalveolar lavage fluid cytology and matrix metalloproteinase-2 and -9 in canine pulmonary eosinophilia. Vet J 163:168–181
7. Hobo T, Yoshihara M, Oikawa M et al (2001) Surfactant proteins in bronchoalveolar lavage fluid of horses: assay technique and changes following road transport. Vet Rec 148:74–80
8. Lakritz J, Marsh AE, Cockrell M et al (2004) Characterization of gelatinases in bronchoalveolar lavage fluid and gelatinases produced by alveolar macrophages isolated from healthy calves. Am J Vet Res 65:163–172
9. Simonen-Jokinen TL, Eskelinen UM, Hartel HM et al (2005) Gelatinolytic matrix metalloproteinases-2 and -9 in tracheobronchial lavage fluid obtained from calves with concurrent infections of *Pasteurella multocida* and *Mycoplasma bovirhinis*. Am J Vet Res 66:2101–2106
10. Birkedal-Hansen H (1995) Proteolytic remodeling of extracellular matrix. Curr Opinion Cell Biol 7:728–735
11. National Research Council (1996) Guide for the Care and Use of Laboratory Animals. National Academy Press, Washington, DC, pp 1–70
12. Bargagli E, Monaci F, Bianchi N et al (2008) Analysis of trace elements in bronchoalveolar lavage of patients with diffuse lung diseases. Biol Trace Elem Res 124(3):225–235
13. Suzuki K, Yamaya Y, Kanzowa N et al (2008) Trace and major elements status in bronchoalveolar lavage fluid in dogs with or without bronchopneumonia. Biol Trace Elem Res 124:92–96
14. Schildge J, Nagel C, Grun C (2007) Bronchoalveolar lavage in interstitial lung diseases: does the recovery rate affect the results? Respiration 74:553–557
15. Higuchi H, Iwano H, Kawai K et al (2011) A simplified PCR assay for fast and easy *Mycoplasma* mastitis screening in dairy cattle. J Vet Sci 12(2):191–193
16. Asano K, Suzuki K, Chiba M et al (2005) Correlation between 25 element contents in mane hair in riding horses and atrioventricular block. Biol Trace Elem Res 108:127–136
17. Akobeng AK (2007) Understanding diagnostic tests 3: receive operating characteristic curves. Acra Paediatrica 96:644–647
18. Hotzel H, Sachse K, Pfützner H (1996) Rapid detection of *Mycoplasma bovis* in milk samples and nasal swabs using the polymerase chain reaction. J Appl Bacteriol 80(5):505–510
19. Nicholas RA, Ayling RD (2003) *Mycoplasma bovis*: disease, diagnosis, and control. Res Vet Sci 74(2):105–112
20. Thompson K, Molina R, Donaghey T et al (2006) The influence of high iron diet on rat lung manganese absorption. Toxicol Appl Pharmacol 210:17–23
21. Marques LM, Buzinhani M, Yamaguti M et al (2007) Use of a polymerase chain reaction for detection of *Mycoplasma dispar* in the nasal mucus of calves. J Vet Diagn Invest 19(1):103–106
22. Chiba M (1994) Bioinorganic chemistry: a science in the spotlight —interface of chemistry, biology, agriculture and medicine. International Journal of PIXE 4:201–216
23. Wu W, Samoszuk MK, Comhair SA et al (2000) Eosinophils generate brominating oxidants in allergen-induced asthma. J Clin Invest 105:1455–1463
24. Brottman GM, Regelmann WE, Slungaard A et al (1996) Effect of eosinophil peroxidase on airway epithelial permeability in the guinea pig. Pediatr Pulmonol 21:159–166
25. Gutteridge JM, Mumby S, Quinlan GJ et al (1996) Pro-oxidant iron is present in human pulmonary epithelial lining fluid: implications for oxidative stress in the lung. Biochem Biophys Res Commun 220:1024–1027
26. Gutteridge JM, Quinlan GJ, Evans TW (2001) The iron paradox of heart and lung and its implications for acute lung injury. Free Radic Res 35:439–443
27. Majeschak M, Sorell LT, Patricelli T et al (2009) Detection and possible role of proteasomes in the bronchoalveolar space of the injured lung. Physiol Res 58(3):363–372
28. Uno D, Tsukagoshi H, Hisada T et al (1997) Effects of the calcium ionophore A23187 on airway responsiveness to histamine and substance P in guinea pigs. Inflamm Res 46:108–113
29. Radi ZA, Kehrli ME Jr, Ackermann MR (2001) Cell adhesion molecules, leukocyte trafficking, and strategies to reduce leukocyte infiltration. J Vet Intern Med 15:516–529
30. Tallant C, Marrero A, Gomis-Rüth FX (2010) Matrix metalloproteinases: fold and function of their catalytic domains. Biochim Biophys Acta 1803(1):20–28

Cell Tissue Res (2012) 347:457–465
DOI 10.1007/s00441-011-1307-2

REGULAR ARTICLE

Distribution and Y397 phosphorylation of focal adhesion kinase on follicular development in the mouse ovary

Masahiro Sakurai · Jun Ohtake · Takayuki Ishikawa · Kentaro Tanemura · Yumi Hoshino · Takahiro Arima · Eimei Sato

Received: 1 April 2011 / Accepted: 12 December 2011 / Published online: 10 February 2012

Abstract Several protein tyrosine kinases (PTKs) are identified as follicle survival factors that suppress apoptosis in granulosa cells. Focal adhesion kinase (FAK/PTK2) interacts with numerous signaling partners and is important for cell adhesion, survival and other vital processes in which FAK autophosphorylation at Y397 (pY397 FAK) is critical for activating signaling pathways. Despite its important roles in apoptosis, the expression and function of FAK in the ovaries remain unknown. Here, we describe FAK expression, including pY397 FAK, in normal healthy mouse ovaries and its association with follicular development and/or atresia. Normal healthy mouse ovaries were used for western blot ($n>60$) and immunohistochemical ($n>180$) analyses. Western blot results in immature and mature mice revealed that total FAK and pY397 FAK were highly expressed in the ovary and immunohistochemistry results in 3-week-old mice showed they were localized to granulosa cells of ovarian follicles, especially preantral follicles. In 3-week-old mice treated with 5 IU pregnant mare serum gonadotropin (for obtaining homogenous populations of growing or atretic follicles), western blotting revealed that follicular atresia progression involved decreased phosphorylation of Y397 at 72 and 96 h after treatment, particularly in granulosa cells of atretic follicles, as shown by immunohistochemistry results at 72 h after treatment. Moreover, immunostaining patterns of FAK and cleaved caspase-3 were negatively correlated in serial sections of 3-week-old mouse ovaries. These results suggest that FAK is most active in ovarian follicle granulosa cells and that its phosphorylation at Y397 is histologically meaningful in follicular development in normal healthy ovaries.

Keywords Ovarian follicular development · Granulosa cells · Apoptosis · Focal adhesion kinase · Phosphorylation

M. Sakurai (✉) · J. Ohtake · T. Ishikawa · K. Tanemura · Y. Hoshino · E. Sato
Laboratory of Animal Reproduction,
Graduate School of Agricultural Science, Tohoku University,
1-1 Amamiya-machi, Tsutsumidori, Aoba-ku,
Sendai, Miyagi 981-8555, Japan
e-mail: sakurai-913@med.tohoku.ac.jp

M. Sakurai · T. Arima
Department of Informative Genetics, Environment and Genome Research Center, Graduate School of Medicine,
Tohoku University,
2-1 Seiryo-machi, Aoba-ku,
Sendai, Miyagi 980-8575, Japan

Introduction

In mammalian ovaries, only a few (<1%) follicles are selected for growth and develop sufficiently for ovulation, whereas most (>99%) follicles undergo a degenerative process known as atresia at various stages in their development (Hirshfield 1991; Tsafriri and Braw 1984). Follicular atresia is initiated as a consequence of the apoptotic cell death of granulosa cells. Subsequently, degeneration of the oocyte occurs at the last stage of atresia (Alonso-Pozos et al. 2003; Manabe et al. 1996) in response to a variety of stimuli in the ovary, including growth factor deprivation (Kaipia and Hsueh 1997), accumulation of metabolites (Tilly 1996) and death signals such as Fas ligand (Sakamaki et al. 1997). While atresia has been extensively studied, the exact mechanisms that direct a follicle towards continued growth or atresia remain unknown.

Several reports have indicated that receptor PTKs are important for regulating the intracellular events that follow stimulation of granulosa cells with various factors. In preovulatory follicles and isolated granulosa cells from rats, the

locally produced survival factors, epidermal growth factor (EGF) and basic fibroblast growth factor (bFGF), the receptors for which possess PTK domains within their molecular structures, suppress apoptosis as effectively as do gonadotropins (Chun et al. 1994; Tilly et al. 1992). Insulin-like growth factor I (IGF-I) has been shown to stimulate the proliferation and steroidogenesis of granulosa cells during *in vitro* culture of cells from different species (Adashi et al. 1985; Erickson et al. 1991; Guthrie et al. 1998).

FAK is a widely expressed 125-kD non-receptor PTK highly enriched in focal adhesions (Hanks and Polte 1997; Schaller et al. 1992). As a key mediator of integrin signaling, FAK is involved in the regulation of cell adhesion, spreading, migration, survival and proliferation (Cary et al. 2002; Schaller 2001; Schaller et al. 1992). Integrin clustering leads to autophosphorylation of FAK at Y397 (Cary et al. 2002), which creates a binding site for the Src-homology 2 (SH2) domain of Src and Fyn (Src family kinases; SFKs) (Cobb et al. 1994; Schaller et al. 1994) as well as phosphatidylinositol 3-kinase (PI3K) (Chen et al. 1996). Following their binding to phosphorylated Y397, SFKs phosphorylate other tyrosine residues in FAK, initiating additional downstream events: phosphorylation at Y576 and Y577 in the catalytic domain increases FAK activity (Calalb et al. 1995; Owen et al. 1999), while binding of PI3K to FAK activates the anti-apoptotic Akt pathway (Chen et al. 1996; Sonoda et al. 2000). In some cells, the SH2 domain of Grb2 binds to phosphorylated Y925 and triggers Ras-dependent activation of the mitogen-activated protein kinase (MAPK) pathway (Schlaepfer et al. 1994; Schlaepfer and Hunter 1996). Therefore, autophosphorylation at Y397 is a key determinant of the physiological functions of FAK.

FAK has been implicated as an important prosurvival factor in the regulation of apoptosis induced by various stimuli; for example, FAK protects cells against apoptosis caused by oxidative stress, etoposide (Sonoda et al. 2000) and ultraviolet light (Chan et al. 1999). Therefore, enhanced FAK signaling may result in uncontrolled proliferation, survival, or migration of cells, as observed in the development and progression of cancers including breast, colon and thyroid carcinomas (Cance et al. 2000; Lark et al. 2003; Owens et al. 1995; Weiner et al. 1993). Several studies (Judson et al. 1999; Sood et al. 2004) have also found that FAK is overexpressed in ovarian cancer cells. In contrast, FAK is proteolytically cleaved and degraded during the early stages of apoptosis in various cell types, including chicken embryo fibroblasts (Crouch et al. 1996) and human umbilical vein endothelial cells (Levkau et al. 1998). Given its involvement in processes important for tumorigenesis and metastasis, FAK might be a promising target in the ongoing search for anticancer drugs in ovarian cancer (Halder et al. 2006); however, the function of FAK in follicular growth and/or atresia in the normal ovary is unknown.

The aims of this study were to determine the expression and localization of FAK in the mouse ovary and to further histologically analyze its relationship to follicular growth and/or atresia. We report the first description of the expression of FAK in the normal healthy mouse ovary and examine the involvement of FAK phosphorylation at Y397 in follicular outcome.

Materials and methods

Animals and collection of ovaries

All ICR mice were purchased from Japan SLC and housed under controlled temperatures (22–27°C) and a constant photoperiod (13L:11D). Mice were provided with a pelleted diet (Oriental Yeast, Japan) and water ad libitum. All investigations were performed in accordance with the Guide for Care and Use of Laboratory Animals of the Graduate School of Agricultural Science, Tohoku University. Virgin female mice 1, 2, 3, 4 and 5 weeks of age were used as immature mice. Estrous cycles of mature mice over 6 weeks of age were tracked by performing daily vaginal smears and only those mice that completed 3 consecutive cycles were used for experiments. Mice were killed by cervical dislocation and then the ovaries were removed and immediately frozen in liquid nitrogen and stored at −80°C for protein extraction or fixed for immunohistochemistry. To synchronize the state of ovarian follicles, immature mice were injected subcutaneously with 5 IU of pregnant mare serum gonadotropin (PMSG; ASKA Pharmaceutical, Japan) at 3 weeks of age. PMSG is known to stimulate growth and development of ovarian follicles for 2 days, after which follicles undergo atresia due to the decline in level of tropic support caused by gonadotropin withdrawal (Dhanasekaran and Moudgal 1989). Therefore, ovaries were collected at 0, 24, 48, 72 and 96 h (defined as P0–P96, respectively) after PMSG treatment; ovaries exhibited homogenous populations of growing follicles at P24 and P48 and atretic follicles at P72 and P96.

SDS-PAGE and western blotting

Total protein from mouse ovaries (4–12 ovaries were pooled in 1 tube per 1 sample) was extracted with RIPA buffer (Cell Signaling Technology, MA, USA) containing 1% (w/v) phenylmethanesulfonyl fluoride (Sigma-Aldrich) and 1% (w/v) phosphatase inhibitor cocktail 1 (Sigma). Total protein from normal 3-week-old mouse lungs (n=3) was used as a positive control. Electrophoresis was performed with 40 μg of total protein in each lane on polyacrylamide gels [8% for

total FAK and FAK phosphorylated at Y397 (pY397 FAK) or 15% for cleaved caspase-3] and the resolved proteins were transferred to polyvinylidene fluoride (PVDF) membranes (Millipore, MA, USA). Thereafter, the membranes were blocked for 1 h at room temperature with Tris-buffered saline (TBS) containing 0.1% Tween 20 (Wako) (TBS-T) and 5% skim milk (Wako Pure Chemical, Japan) or 5% albumin from bovine serum (BSA; Sigma) for the detection of total FAK and cleaved caspase-3 or pY397 FAK, respectively. After 3 washes with TBS-T, membranes were incubated with rabbit anti-total FAK monoclonal antibody (diluted 1:1,000; Abcam, UK), rabbit anti-pY397 FAK monoclonal antibody (1:4,000; Invitrogen), rabbit anti-cleaved caspase-3 monoclonal antibody (1:1,000; Cell Signaling Technology), or mouse anti-α-tubulin monoclonal antibody (for α-tubulin as a loading control, 1:2,000; Sigma) overnight at 4°C. After 3 washes, the membranes were reacted with horseradish peroxidase-conjugated goat anti-rabbit IgG (diluted 1:15,000 for total FAK, 1:20,000 for pY397 FAK and 1:10,000 for cleaved caspase-3; Jackson Immuno Research, PA, USA) or horseradish peroxidase-conjugated goat anti-mouse IgG (1:40,000 for α-tubulin; Sigma) for 1 h at room temperature. Peroxidase activity was visualized using the ECL Plus western blotting detection system (GE Healthcare, UK).

Statistical analysis

Western blot analyses were repeated at least three times. The densitometric ratios of the bands representing total FAK and pY397 FAK relative to that for α-tubulin, as well as pY397/total FAK ratio, were analyzed using Student's *t* test. $P< 0.05$ was considered statistically significant.

Immunohistochemistry

Ovaries collected from 3-week-old mice with or without PMSG injection (at P48 and P72) (each treatment, $n> 60$), from mature mice (each estrous cycle: $n=3$), or lungs from 3-week-old mice used as positive controls ($n=3$), were fixed for 4 h at room temperature in 10% formalin (v/v; Wako) containing 1% phosphatase inhibitor cocktail 1 in Ca^{2+}- and Mg^{2+}-free Dulbecco's phosphate-buffered saline (PBS; Nissui Pharmaceutical;, Japan), after which they were dehydrated, embedded in paraffin, serially sectioned (4–7 μm thick) and mounted on Matsunami adhesive silane (MAS)-coated glass slides (Matsunami Glass, Japan). Sections were deparaffinized and rehydrated. For antigen retrieval, sections were exposed for 10 min to boiling 10 mM trisodium citrate dihydrate (pH 6.0; Wako) containing 0.05% Tween 20 and washed twice in PBS. Sections were incubated for 20 min with 3% H_2O_2 (Wako) in methanol (Wako) to eliminate endogenous peroxidase activity prior to washing twice with PBS. In order to block nonspecific protein binding, sections were incubated with 5% BSA in PBS for 30 min and washed twice with PBS. Sections were then incubated with rabbit anti-total FAK monoclonal antibody (diluted 1:50), rabbit anti-pY397 FAK monoclonal antibody (1:200), rabbit anti-cleaved caspase-3 monoclonal antibody (1:100), or rabbit monoclonal isotype control (1:50; Cell Signaling Technology) overnight at 4°C (for total FAK, cleaved caspase-3 and isotype control staining) or for 1 h at room temperature (for pY397 FAK staining). Following washing twice with PBS, sections were next reacted with biotinylated anti-rabbit IgG (diluted 1:100 for total FAK, 1:400 for pY397 FAK, 1:200 for cleaved caspase-3 and 1:100 for isotype control staining; Vector Laboratories, CA, USA) for 30 min. Washed twice with PBS, finally, sections were incubated with peroxidase-conjugated streptavidin (Nichirei, Japan) for 10 min. After 2 washes with PBS, slides were developed by incubation with 3,3′-diaminobenzidine tetrahydrochloride (DAB; Vector Laboratories) until color development was noted; the color reaction was stopped by washing the slides in distilled water. The sections were counterstained with hematoxylin (Wako) and then mounted with Fluoromount-G (SouthernBiotech, AL, USA).

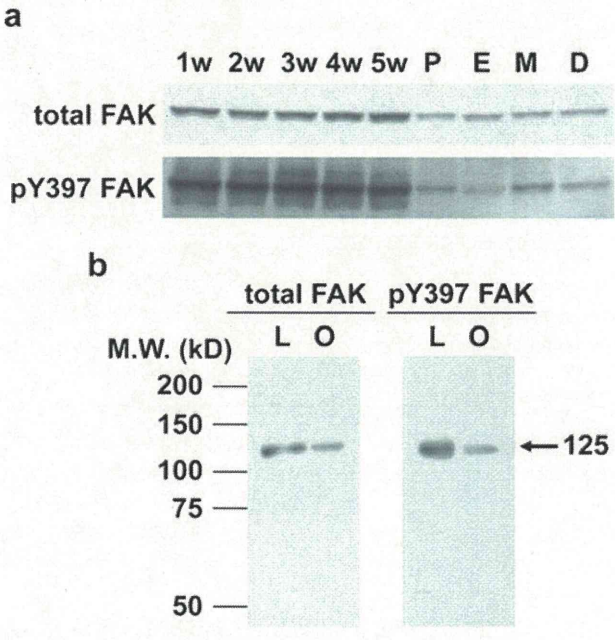

Fig. 1 **a** Expression of total FAK and pY397 FAK in mouse ovaries. **b** Expression of total FAK and pY397 FAK in mouse lungs used as positive controls. The molecular weights of total FAK and pY397 FAK in normal healthy ovaries and lungs from 3-week-old mice were identical. *1w–5w* 1- to 5-week-old, *P* proestrus, *E* estrus, *M* metestrus, *D* diestrus, *L* lung, *O* Ovary, *M.W.* molecular weight

Results

Expression levels of total and pY397 FAK in the mouse ovary

Western blot analysis was performed to investigate whether total FAK and pY397 FAK were expressed in normal healthy mouse ovaries. Both total and pY397 FAK were highly expressed in ovaries from immature mice and expression levels did not change significantly with age. In contrast, expression levels of total and pY397 FAK were lower in the ovaries of mature mice than in those of immature mice, although the expression levels in mature mice were similar during estrous cycle (Fig. 1a).

Localization of total and pY397 FAK in ovaries

To investigate the localization of FAK in the mouse ovary, immunohistochemical studies were performed on ovaries from 3-week-old and mature mice. As shown in Fig. 2a–d, total FAK was expressed at high levels in the granulosa cells of ovarian follicles at every developmental stage, from primordial to antral follicles. Low levels of total FAK were observed in oocytes, very low levels were observed in theca cells and FAK levels were undetectable in basement membranes. In the ovaries collected from mature mice during diestrus, total FAK was also expressed in the corpus luteum (CL) at low levels (Fig. 2e). The expression pattern of total

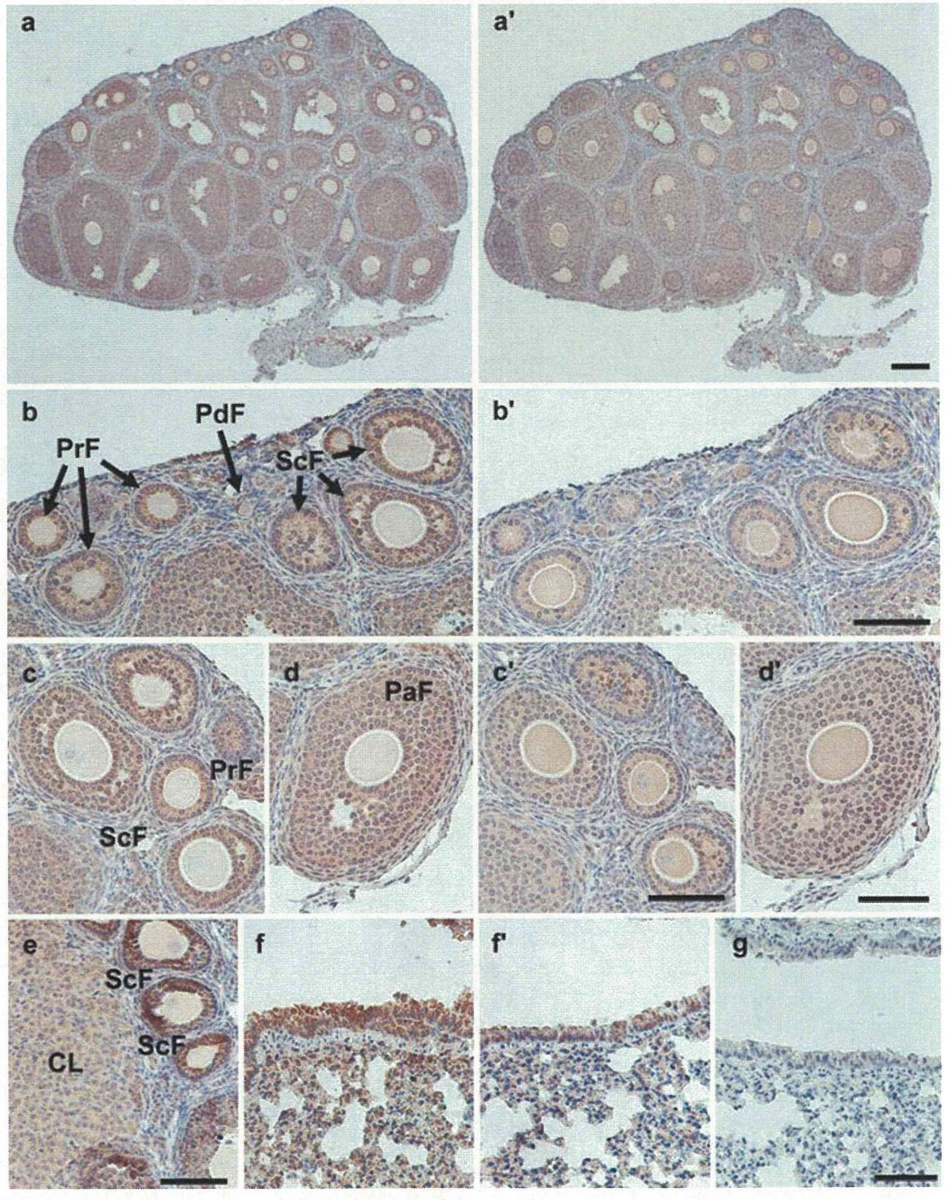

Fig. 2 Distributions of total FAK and pY397 FAK in normal healthy mouse ovaries. Serial sections (**a**–**e**) and (**a′**–**d′**) were stained for total (**a**–**e**) and pY397 (**a′**–**d′**) FAK and visualized with DAB (*brown*). The distributions of total and pY397 FAK were similar and total and pY397 FAK were expressed strongly in granulosa cells in follicles at all developmental stages and weakly in the corpus luteum. **a**–**d** and **e** are ovarian sections from 3-week-old mice or mature mice during diestrus, respectively. **a** Low magnification, **b** primordial to secondary follicles, **c** primary to secondary (early preantral) follicles, **d** preantral (early antral) follicles. Immature mouse lungs were used to examine positive (**f**, **f′**) and negative (**g**) control reactions to total FAK and pY397 FAK. In the lung, total and pY397 FAK were expressed in the bronchial epithelium. *PdF* primordial follicles, *PrF* primary follicles, *ScF* secondary follicles, *PaF* preantral follicles, *CL* corpus luteum. *Bars* 100 μm

FAK was similar at each stage of the estrous cycle. Moreover, immunostaining of serial sections for total and pY397 FAK indicated that pY397 FAK, like total FAK, was highly expressed in the granulosa cells in follicles at every developmental stage, as well as in the oocytes; granulosa cells that were positive for total FAK also expressed pY397 FAK (Fig. 2a′–d′).

Expression levels of total and pY397 FAK in hormonally regulated ovaries

To clarify the relationship between expression levels of FAK and follicular growth and/or atresia, PMSG injection was performed to obtain homogenous populations of growing or atretic follicles and then expression levels of total and pY397 FAK at P24, 48, 72 and 96 were compared with those at P0 by western blotting analysis using Student's *t* test (Fig. 3a); the same statistical significances were obtained also using one-way ANOVA, followed by Fisher's protected least significant differences (PLSD) test (data not shown). The expression level of total FAK tended to be lower after PMSG treatment but was significantly lower only at P72 compared with P0 (Fig. 3b). In contrast, the expression level of pY397 FAK was significantly lower from P24 to P96 compared with P0 (Fig. 3b). To examine these expression levels more clearly, the pY397/total FAK ratio was also statistically analyzed. It was observed that the pY397/total FAK ratio was significantly decreased at P72 and P96 (Fig. 3b), when ovaries exhibited homogenous populations of atretic follicles as demonstrated by an increase in concentration of active fragments of caspase-3; cleaved caspase-3 (an indicator of progressing follicular atresia) (Fig. 3a).

Localization of total and pY397 FAK in hormonally regulated ovaries

Many fully grown antral follicles were present in ovaries 48 h after PMSG injection (Fig. 4a). In large antral follicles, total and pY397 FAK were expressed in cumulus cells and granulosa cells, especially those proximate to the antrum (Fig. 4b–c′). The expression levels of FAK were higher in the granulosa cells of preantral follicles than in those of antral follicles (Fig. 4b). In the ovaries that exhibited homogenous populations of atretic follicles and CLs at P72 (Fig. 5a and a′), the expression level of pY397 FAK was low in the granulosa cells of follicles at the early stage of atresia, containing pyknotic (apoptotic) cells; however, total FAK was highly expressed in the same cells, as shown in immunostained serial sections (Figs. 5b and b′).

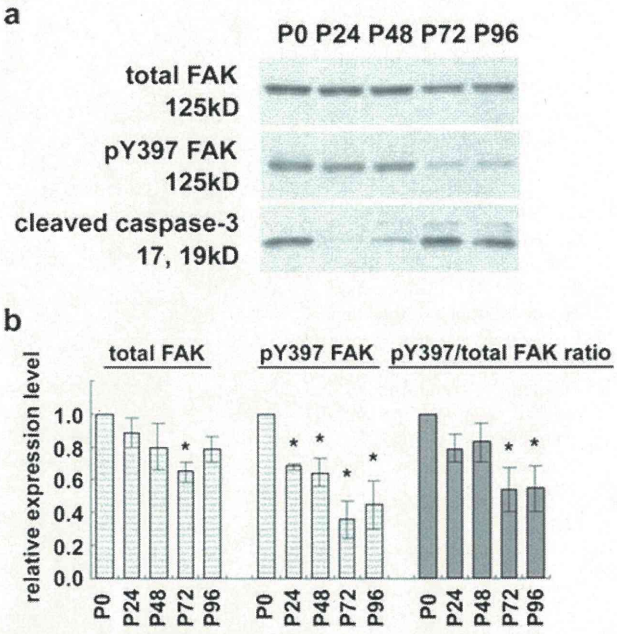

Fig. 3 **a** Expression of total FAK and pY397 FAK and detection of cleaved caspase-3 in ovaries from PMSG-injected mice. **b** Relative expression levels of total FAK and pY397 FAK. Values are mean ± SEM (n=3). Significant differences (P<0.05) in comparison to P0 are indicated by *asterisks*. P0–P96, times (h) after PMSG injection

Relevance to apoptosis

Follicular atresia is initiated by the apoptosis of granulosa cells. Therefore, we finally examined the relevance of FAK expression to apoptotic events in granulosa cells by immunostaining serial sections of mouse ovaries for total FAK, pY397 FAK and cleaved capsase-3. As shown in Fig. 6, intact granulosa cells expressed both total and pY397 FAK but were negative for cleaved caspase-3. In contrast, pyknotic granulosa cells were negative for total and pY397 FAK but showed intense cleaved caspase-3 staining. These results indicate that FAK expression decreased in apoptotic granulosa cells, which coincides with the cleavage of FAK by activated caspase-3 during apoptosis. Unexpected total FAK expression in apoptotic cell debris may represent the condensed cleaved products of FAK by activated caspase-3.

Discussion

The granulosa and theca cells in the ovary release local factors such as cytokines (Adashi 1992) and various growth factors (Adashi et al. 1991; Roy and Greenwald 1996), which regulate the growth of ovarian follicles via autocrine and/or paracrine mechanisms. Furthermore, phosphorylation of intracellular signaling molecules by PTKs is essential for

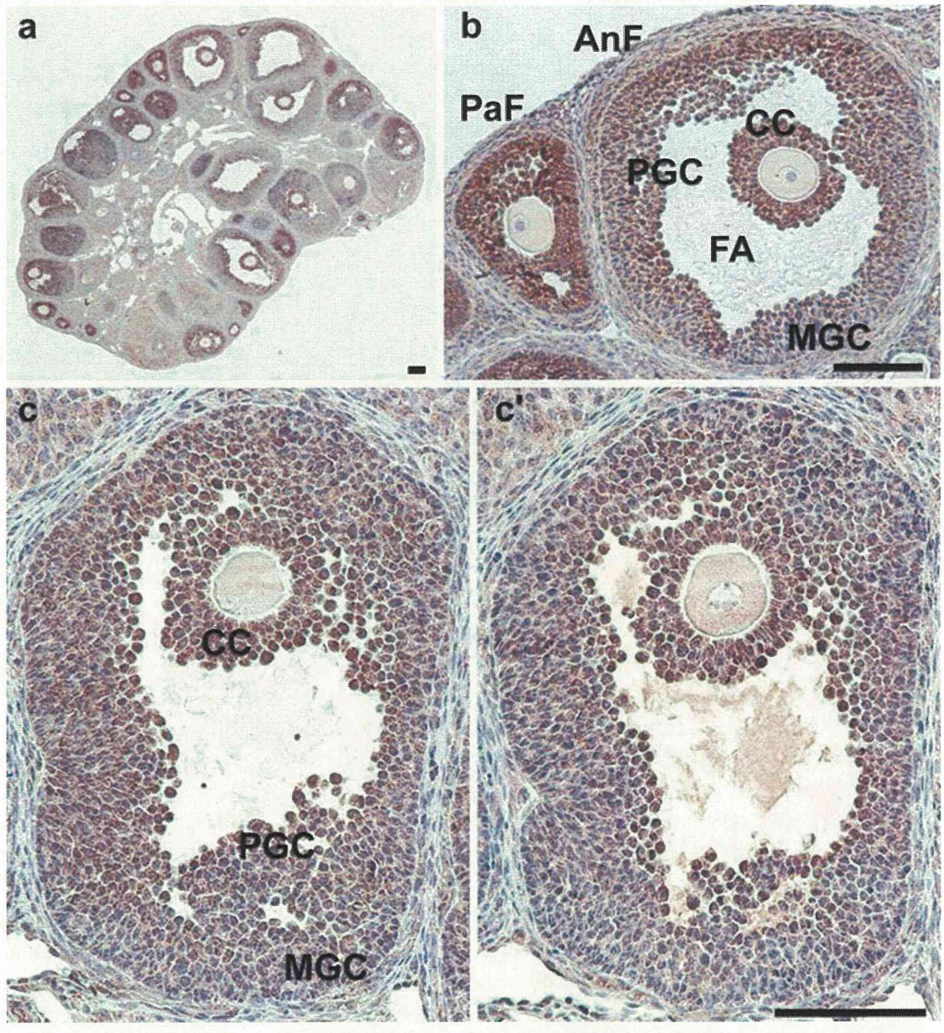

Fig. 4 Distributions of total FAK and pY397 FAK in mouse ovaries at 48 h after PMSG treatment. **a**, **b** Immunostained total FAK was visualized with DAB (*brown*). Total FAK was strongly expressed in cumulus cells and periantral granulosa cells of antral follicles. Serial sections (**c**, **c'**), were stained for total and pY397 FAK and visualized with DAB (*brown*). The distributions of total and Y397 FAK were similar in antral follicles. *PaF* preantral follicle, *AnF* antral follicle, *CC* cumulus cells, *PGC* periantral granulosa cells, *MGC* membrana granulosa cells, *FA* follicular antrum. **a** Low magnification; **b** high magnification image of (**a**). *Bars* 100 μm

regulating the dynamics of follicular growth and atresia (Chun et al. 1994, 1996; Dissen et al. 2001; Tilly et al. 1992).

In the mouse ovary, the total FAK and pY397 FAK (hereafter together called FAKs) expression levels were similar during immature development and estrous cycles; however, FAK expression levels in the ovaries of mature mice were lower than those of immature mice (Fig. 1a). Total ovary lysates were used for western blot analyses; immunohistochemistry results showed that FAKs were expressed at low levels in CLs (Fig. 2e), which may explain the decrease of FAKs in whole ovaries of mature mice, because CL accounts for a large part of the whole ovary in mature mice.

In this study, a strong expression of both total and pY397 FAK was observed in the granulosa cells of ovarian follicles (Fig. 2), which is consistent with the known roles of FAK in cell adhesion, spreading, migration, survival and proliferation in various cell types (Cary and Guan 1999; Schaller 2001; Schaller et al. 1992). This suggests that total FAK, including pY397 FAK, is histologically involved in the functioning of granulosa cells, such as cellular survival and proliferation. However, whether follicles that express FAKs continue to grow or undergo atresia or, in other words, whether FAKs play a positive or negative role in follicular development is unclear.

To examine the relationship between FAKs and follicular growth and/or atresia, we used ovaries containing homogenous populations of growing or atretic follicles from PMSG-injected mice. Before PMSG injection (P0), FAKs were highly expressed and active fragments of caspase-3 were also strongly detected. At P24 and P48, cleaved caspase-3 concentration drastically decreased (Fig. 3a); because of the anti-apoptotic effects of PMSG, total FAK expression levels were unexpectedly lower and that of pY397 FAK were significantly lower. Because the pY397/total FAK ratio did not significantly decrease at P24 and P48, it was suggested that the significant decrease in pY397 FAK expression at these time points was due to the decrease in total FAK expression. The decrease in total FAK expression coincided with the lower FAK expression in granulosa cells of antral

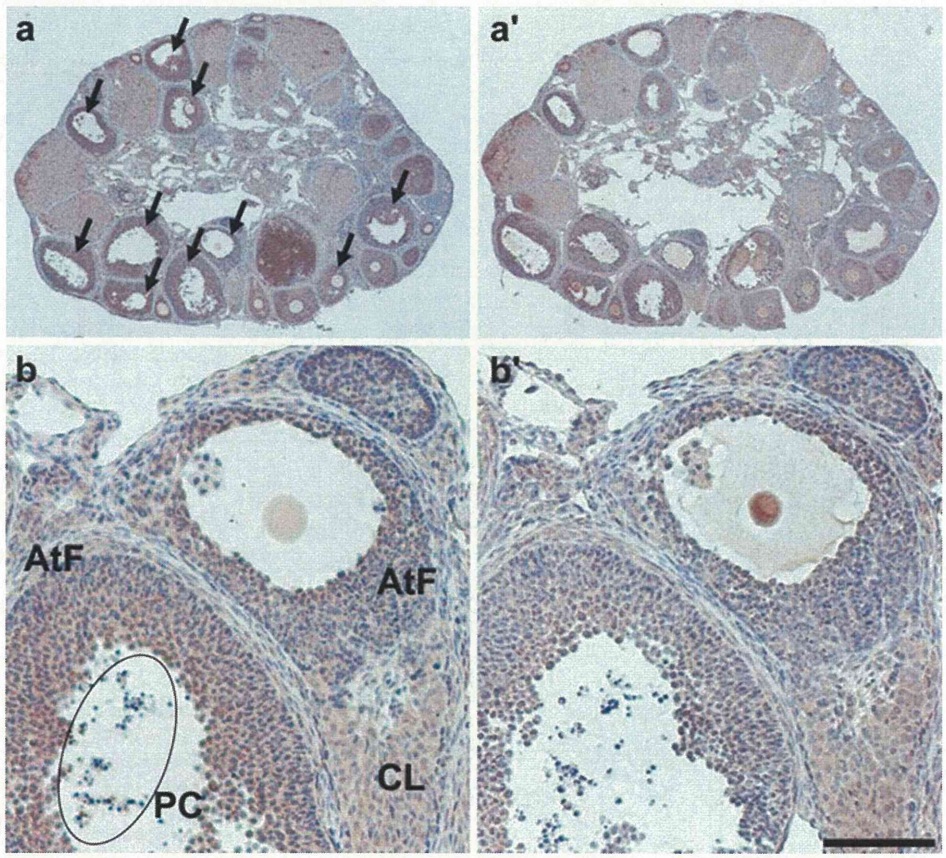

Fig. 5 Distributions of total FAK and pY397 FAK in mouse ovaries at 72 h after PMSG treatment. Serial sections, (**a**, **b**) and (**a′**, **b′**), were stained for total (**a**, **b**) and pY397 (**a′**, **b′**) FAK and visualized with DAB (*brown*). Expression of pY397 FAK was low in the granulosa cells of atretic follicles. *AtF* atretic follicle, *CL* corpus luteum, *PC* pyknotic (apoptotic) cells. **b** and **b′** are high magnification images of (**a**) and (**a′**), respectively. *Arrows* indicate atretic follicles including pyknotic (apoptotic) cells. *Bar* 100 μm

follicles as compared to that in preantral follicles, which account for a large portion of the ovary (Fig. 4). Most importantly, the total FAK and pY397 FAK expression levels were significantly lower at P72 than at P0 (Fig. 3b). This significant decrease in pY397 FAK expression cannot be explained only by the decreased total FAK expression, because the pY397/total FAK ratio was also significantly low at this time point (Fig. 3b). A significant decrease in total FAK might be because of its very low expression in many follicles at late stages of atresia as well as its low expression in the CLs. At P72, cleaved caspase-3 was strongly detected (Fig. 3a); furthermore, pY397 FAK was expressed at a low level in granulosa cells of large follicles at early stage of atresia (Fig. 5b′). Phosphorylated Y397 is a docking site for PI3K (Chen et al. 1996), which activates the anti-apoptotic Akt pathway (Sonoda et al. 2000). Moreover, the apoptotic events triggered by FAK deactivation are accompanied by rapid FAK dephosphorylation at Y397, endogenous FAK degradation and caspase-3 activation (Beviglia et al. 2003). Proliferation and differentiation of granulosa cells are the essence of ovarian follicular development (Simpson et al. 2002) and the FAK expression was especially strong in undifferentiated follicular granulosa cells at preantral stages (Fig. 4b). Therefore, our results suggest that FAK phosphorylation

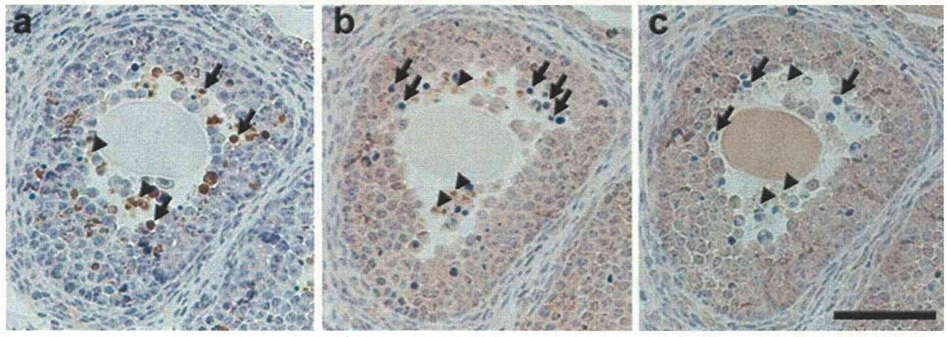

Fig. 6 Relevance of FAK to apoptosis of granulosa cells. Serial sections of ovaries from 3-week-old mice were stained for cleaved caspase-3 (**a**), total FAK (**b**) and pY397 FAK (**c**) and visualized with DAB (*brown*). *Arrows* and *arrowheads* indicate pyknotic cells and apoptotic cell debris, respectively. *Bar* 50 μm

at Y397 has a positive role in follicular growth by promoting the proliferation and survival of granulosa cells.

In serially sectioned specimens, we compared the total FAK and pY397 FAK expression patterns with immunolocalization of cleaved caspase-3 to examine the role of FAKs in granulosa cell apoptosis (Fig. 6). Active fragments of caspase-3 were strongly localized in some granulosa cells of ovaries collected from 3-week-old mice and FAKs were not expressed in pyknotic cells that are positive for cleaved caspase-3 staining. FAK is cleaved by activated caspase-3 (Wen et al. 1997) and this cleavage coincides with the loss of FAK from focal contacts, cell rounding and redistribution of FAK to characteristic apoptotic membrane protrusions (Levkau et al. 1998). FAK has also been demonstrated to suppress apoptosis by binding to receptor-interacting protein, which is essential for the formation of the death-inducing signaling complex (Takahashi et al. 2007). As early follicular atresia is characterized by a small degree of apoptosis in granulosa cells, this result further confirms that FAKs histologically play positive roles in granulosa cell survival, which is important for ovarian follicular development.

In antral follicles, granulosa cells differentiated into 3 distinct phenotypes—cumulus, periantral and membrana granulosa cells—based on their position relative to oocytes, which is dictated by the concentration of morphogens secreted from oocytes, including growth differentiation factor 9 and bone morphogenetic protein (BMP) 15 (Erickson and Shimasaki 2000). These morphogens promote growth and prevent apoptosis of cumulus cells (Gilchrist et al. 2004; Hussein et al. 2005). Moreover, a BMP gradient was suggested to be responsible for the mechanism whereby follicular atresia was initiated from granulosa cells (Hussein et al. 2005). FAKs were also localized to oocytes and cumulus cells and expression of their gradients was observed in granulosa cell layers (Fig. 4). Thus, the FAK function in the cumulus and granulosa cells may be regulated by the oocyte-secreted morphogens. Considering that oocytes and granulosa cells are morphologically and physiologically different (e.g., oocytes do not proliferate and migrate within the follicle), the role of FAK in oocytes may differ from that in granulosa cells. Therefore, FAK may have other functions in the ovary, in addition to follicular development, which are predicted to resemble those of other PTKs, e.g., IGF-I and its receptor, which regulate oocyte meiotic maturation (Yoshimura et al. 1996), cumulus cell expansion (Singh and Armstrong 1997), as well as granulosa cell proliferation (Zhou et al. 1991).

In this study, we demonstrated that FAK is strongly expressed in granulosa cells of growing follicles, particularly at the preantral stage, in normal healthy mouse ovaries and that especially its phosphorylated form at Y397 supports follicular development by inducing survival and proliferation of granulosa cells.

Acknowledgement This work was supported by the Japan Society for the Promotion of Science Grant to E. Sato (No. 21248032).

References

Adashi EY (1992) The potential relevance of cytokines to ovarian physiology. J Steroid Biochem Mol Biol 43:439–444

Adashi EY, Resnick CE, D'Ercole AJ, Svoboda ME, Van Wyk JJ (1985) Insulin-like growth factors as intraovarian regulators of granulosa cell growth and function. Endocr Rev 6:400–420

Adashi EY, Resnick CE, Vera A, Hernandez ER (1991) In vivo regulation of granulosa cell type I insulin-like growth factor receptors: evidence for an inhibitory role for the putative endogenous ligand(s) of the ovarian gonadotropin-releasing hormone receptor. Endocrinology 128:3130–3137

Alonso-Pozos I, Rosales-Torres AM, Avalos-Rodriguez A, Vergara-Onofre M, Rosado-Garcia A (2003) Mechanism of granulosa cell death during follicular atresia depends on follicular size. Theriogenology 60:1071–1081

Beviglia L, Golubovskaya V, Xu L, Yang X, Craven RJ, Cance WG (2003) Focal adhesion kinase N-terminus in breast carcinoma cells induces rounding, detachment and apoptosis. Biochem J 373:201–210

Calalb MB, Polte TR, Hanks SK (1995) Tyrosine phosphorylation of focal adhesion kinase at sites in the catalytic domain regulates kinase activity: a role for Src family kinases. Mol Cell Biol 15:954–963

Cance WG, Harris JE, Iacocca MV, Roche E, Yang X, Chang J, Simkins S, Xu L (2000) Immunohistochemical analyses of focal adhesion kinase expression in benign and malignant human breast and colon tissues: correlation with preinvasive and invasive phenotypes. Clin Cancer Res 6:2417–2423

Cary LA, Guan JL (1999) Focal adhesion kinase in integrin-mediated signaling. Front Biosci 4:D102–113

Cary LA, Klinghoffer RA, Sachsenmaier C, Cooper JA (2002) SRC catalytic but not scaffolding function is needed for integrin-regulated tyrosine phosphorylation, cell migration, and cell spreading. Mol Cell Biol 22:2427–2440

Chan PC, Lai JF, Cheng CH, Tang MJ, Chiu CC, Chen HC (1999) Suppression of ultraviolet irradiation-induced apoptosis by overexpression of focal adhesion kinase in Madin-Darby canine kidney cells. J Biol Chem 274:26901–26906

Chen HC, Appeddu PA, Isoda H, Guan JL (1996) Phosphorylation of tyrosine 397 in focal adhesion kinase is required for binding phosphatidylinositol 3-kinase. J Biol Chem 271:26329–26334

Chun SY, Billig H, Tilly JL, Furuta I, Tsafriri A, Hsueh AJ (1994) Gonadotropin suppression of apoptosis in cultured preovulatory follicles: mediatory role of endogenous insulin-like growth factor I. Endocrinology 135:1845–1853

Chun SY, Eisenhauer KM, Minami S, Billig H, Perlas E, Hsueh AJ (1996) Hormonal regulation of apoptosis in early antral follicles: follicle-stimulating hormone as a major survival factor. Endocrinology 137:1447–1456

Cobb BS, Schaller MD, Leu TH, Parsons JT (1994) Stable association of pp 60src and pp59fyn with the focal adhesion-associated protein tyrosine kinase, pp125FAK. Mol Cell Biol 14:147–155

Crouch DH, Fincham VJ, Frame MC (1996) Targeted proteolysis of the focal adhesion kinase pp 125 FAK during c-MYC-induced apoptosis is suppressed by integrin signalling. Oncogene 12:2689–2696

Dhanasekaran N, Moudgal NR (1989) Biochemical and histological validation of a model to study follicular atresia in rats. Endocrinol Exp 23:155–166

Dissen GA, Romero C, Hirshfield AN, Ojeda SR (2001) Nerve growth factor is required for early follicular development in the mammalian ovary. Endocrinology 142:2078–2086

Erickson GF, Shimasaki S (2000) The role of the oocyte in folliculogenesis. Trends Endocrinol Metab 11:193–198

Erickson GF, Garzo VG, Magoffin DA (1991) Progesterone production by human granulosa cells cultured in serum free medium: effects of gonadotrophins and insulin-like growth factor I (IGF-I). Hum Reprod 6:1074–1081

Gilchrist RB, Ritter LJ, Armstrong DT (2004) Oocyte-somatic cell interactions during follicle development in mammals. Anim Reprod Sci 82–83:431–446

Guthrie HD, Garrett WM, Cooper BS (1998) Follicle-stimulating hormone and insulin-like growth factor-I attenuate apoptosis in cultured porcine granulosa cells. Biol Reprod 58:390–396

Halder J, Kamat AA, Landen CN Jr, Han LY, Lutgendorf SK, Lin YG, Merritt WM, Jennings NB, Chavez-Reyes A, Coleman RL, Gershenson DM, Schmandt R, Cole SW, Lopez-Berestein G, Sood AK (2006) Focal adhesion kinase targeting using in vivo short interfering RNA delivery in neutral liposomes for ovarian carcinoma therapy. Clin Cancer Res 12:4916–4924

Hanks SK, Polte TR (1997) Signaling through focal adhesion kinase. Bioessays 19:137–145

Hirshfield AN (1991) Development of follicles in the mammalian ovary. Int Rev Cytol 124:43–101

Hussein TS, Froiland DA, Amato F, Thompson JG, Gilchrist RB (2005) Oocytes prevent cumulus cell apoptosis by maintaining a morphogenic paracrine gradient of bone morphogenetic proteins. J Cell Sci 118:5257–5268

Judson PL, He X, Cance WG, Van Le L (1999) Overexpression of focal adhesion kinase, a protein tyrosine kinase, in ovarian carcinoma. Cancer 86:1551–1556

Kaipia A, Hsueh AJ (1997) Regulation of ovarian follicle atresia. Annu Rev Physiol 59:349–363

Lark AL, Livasy CA, Calvo B, Caskey L, Moore DT, Yang X, Cance WG (2003) Overexpression of focal adhesion kinase in primary colorectal carcinomas and colorectal liver metastases: immunohistochemistry and real-time PCR analyses. Clin Cancer Res 9:215–222

Levkau B, Herren B, Koyama H, Ross R, Raines EW (1998) Caspase-mediated cleavage of focal adhesion kinase pp 125FAK and disassembly of focal adhesions in human endothelial cell apoptosis. J Exp Med 187:579–586

Manabe N, Imai Y, Ohno H, Takahagi Y, Sugimoto M, Miyamoto H (1996) Apoptosis occurs in granulosa cells but not cumulus cells in the atretic antral follicles in pig ovaries. Experientia 52:647–651

Owen JD, Ruest PJ, Fry DW, Hanks SK (1999) Induced focal adhesion kinase (FAK) expression in FAK-null cells enhances cell spreading and migration requiring both auto- and activation loop phosphorylation sites and inhibits adhesion-dependent tyrosine phosphorylation of Pyk2. Mol Cell Biol 19:4806–4818

Owens LV, Xu L, Craven RJ, Dent GA, Weiner TM, Kornberg L, Liu ET, Cance WG (1995) Overexpression of the focal adhesion kinase (p125FAK) in invasive human tumors. Cancer Res 55:2752–2755

Roy SK, Greenwald GS (1996) Follicular development through preantral stages: signalling via growth factors. J Reprod Fertil Suppl 50:83–94

Sakamaki K, Yoshida H, Nishimura Y, Nishikawa S, Manabe N, Yonehara S (1997) Involvement of Fas antigen in ovarian follicular atresia and luteolysis. Mol Reprod Dev 47:11–18

Schaller MD (2001) Biochemical signals and biological responses elicited by the focal adhesion kinase. Biochim Biophys Acta 1540:1–21

Schaller MD, Borgman CA, Cobb BS, Vines RR, Reynolds AB, Parsons JT (1992) pp 125FAK a structurally distinctive protein-tyrosine kinase associated with focal adhesions. Proc Natl Acad Sci USA 89:5192–5196

Schaller MD, Hildebrand JD, Shannon JD, Fox JW, Vines RR, Parsons JT (1994) Autophosphorylation of the focal adhesion kinase, pp 125FAK, directs SH2-dependent binding of pp60src. Mol Cell Biol 14:1680–1688

Schlaepfer DD, Hunter T (1996) Evidence for in vivo phosphorylation of the Grb2 SH2-domain binding site on focal adhesion kinase by Src-family protein-tyrosine kinases. Mol Cell Biol 16:5623–5633

Schlaepfer DD, Hanks SK, Hunter T, van der Geer P (1994) Integrin-mediated signal transduction linked to Ras pathway by GRB2 binding to focal adhesion kinase. Nature 372:786–791

Simpson ER, Clyne C, Rubin G, Boon WC, Robertson K, Britt K, Speed C, Jones M (2002) Aromatase–a brief overview. Annu Rev Physiol 64:93–127

Singh B, Armstrong DT (1997) Insulin-like growth factor-1, a component of serum that enables porcine cumulus cells to expand in response to follicle-stimulating hormone in vitro. Biol Reprod 56:1370–1375

Sonoda Y, Matsumoto Y, Funakoshi M, Yamamoto D, Hanks SK, Kasahara T (2000) Anti-apoptotic role of focal adhesion kinase (FAK). Induction of inhibitor-of-apoptosis proteins and apoptosis suppression by the overexpression of FAK in a human leukemic cell line, HL-60. J Biol Chem 275:16309–16315

Sood AK, Coffin JE, Schneider GB, Fletcher MS, DeYoung BR, Gruman LM, Gershenson DM, Schaller MD, Hendrix MJ (2004) Biological significance of focal adhesion kinase in ovarian cancer: role in migration and invasion. Am J Pathol 165:1087–1095

Takahashi R, Sonoda Y, Ichikawa D, Yoshida N, Eriko AY, Tadashi K (2007) Focal adhesion kinase determines the fate of death or survival of cells in response to TNFalpha in the presence of actinomycin D. Biochim Biophys Acta 1770:518–526

Tilly JL (1996) Apoptosis and ovarian function. Rev Reprod 1:162–172

Tilly JL, Billig H, Kowalski KI, Hsueh AJ (1992) Epidermal growth factor and basic fibroblast growth factor suppress the spontaneous onset of apoptosis in cultured rat ovarian granulosa cells and follicles by a tyrosine kinase-dependent mechanism. Mol Endocrinol 6:1942–1950

Tsafriri A, Braw RH (1984) Experimental approaches to atresia in mammals. Oxf Rev Reprod Biol 6:226–265

Weiner TM, Liu ET, Craven RJ, Cance WG (1993) Expression of focal adhesion kinase gene and invasive cancer. Lancet 342:1024–1025

Wen LP, Fahrni JA, Troie S, Guan JL, Orth K, Rosen GD (1997) Cleavage of focal adhesion kinase by caspases during apoptosis. J Biol Chem 272:26056–26061

Yoshimura Y, Ando M, Nagamatsu S, Iwashita M, Adachi T, Sueoka K, Miyazaki T, Kuji N, Tanaka M (1996) Effects of insulin-like growth factor-I on follicle growth, oocyte maturation, and ovarian steroidogenesis and plasminogen activator activity in the rabbit. Biol Reprod 55:152–160

Zhou J, Chin E, Bondy C (1991) Cellular pattern of insulin-like growth factor-I (IGF-I) and IGF-I receptor gene expression in the developing and mature ovarian follicle. Endocrinology 129:3281–3288

Biochemical and Biophysical Research Communications 415 (2011) 691–695

Contents lists available at SciVerse ScienceDirect

Biochemical and Biophysical Research Communications

journal homepage: www.elsevier.com/locate/ybbrc

Adrenomedullin: A possible regulator of germinal vesicle breakdown

Yuuki Hiradate *, Jun Ohtake, Yumi Hoshino, Kentaro Tanemura, Eimei Sato

Laboratory of Animal Reproduction, Graduate School of Agricultural Science, Tohoku University, 1-1 Tsutsumidori-Amamiyamachi Aobaku, Sendai 981-8555, Japan

ARTICLE INFO

Article history:
Received 25 October 2011
Available online 4 November 2011

Keywords:
Adrenomedullin
Nitric oxide
Cumulus cell
GVBD
Akt

ABSTRACT

Adrenomedullin (ADM) is a multifunctional hormone that regulates processes as diverse as blood pressure and cell growth. Although expressed in the ovary, the role of ADM in this organ is not clear. In the present study, we found the expression of ADM receptor and receptor activity-modifying proteins in mouse cumulus cells but not in the oocytes. We report that germinal vesicle breakdown (GVBD), which is required for oocyte maturation, is not inhibited by ADM alone. However, ADM in the presence of the nitric oxide donor sodium nitroprusside (SNP) significantly inhibited GVBD. Furthermore, the ADM- and SNP-dependent inhibition of GVBD was abrogated by Akt blockade. Additionally, Akt expression and phosphorylation was exhibited by ADM, suggesting that Akt signaling upstream in cumulus cells is responsible. Additionally, immunohistochemical analysis revealed that ADM was localized in the granulosa cells of developed follicles, implying the possibility that ADM physiologically affects oocyte maturation *in vivo*. Our results provide the evidence that ADM can act as a GVBD regulator.

1. Introduction

In mammalian reproductive systems, oocyte meiosis is arrested within the ovarian follicles at the diplotene stage of the first meiotic prophase – this is termed as meiotic arrest. During the meiotic arrest phase, the intact nuclear membrane forms a characteristic germinal vesicle (GV) [1]. Once signal transduction is triggered by gonadotropin in cumulus cells surrounding the oocyte, GV breakdown (GVBD) is induced and meiosis is reactivated (so-called "meiotic resumption") [1]. The oocyte is then competent for fertilization until it reaches metaphase II. Oocytes isolated from immature antral follicles prior to the GV stage are incapable of completing meiosis and require further growth to acquire developmental competence [2]. This phenomenon has led to the proposal that additional processes at the GV stage are required for oocyte maturation.

Intriguingly, because mammalian oocytes cultured *in vitro* undergo spontaneous GVBD, it has been suggested that an inhibitor of meiotic resumption is present *in vivo* [3]. Several factors have been associated with GVBD inhibition, suggesting that the process is not under the control of a single "master regulator." In the present study, we have identified additional factors that can modulate meiotic resumption.

Adrenomedullin (ADM) is a pluripotent peptide isolated from a human pheochromocytoma [4] and consists of 50 amino acids in rats and mice. The ADM receptor, known as a calcitonin receptor-like receptor (CRLR), requires the co-expression of modifiers known as receptor activity modifying proteins (RAMPs) [5]. Co-expression of CRLR with RAMP-1 reconstitutes a calcitonin gene-related peptide receptor, whereas co-expression with RAMP-2 or RAMP-3 functions as an ADM receptor. ADM is expressed in many tissues and has various physiological functions, including regulation of blood pressure [4], angiogenesis [6], and cell growth [7].

Although recent studies have shown that ADM is expressed in the rat and human ovary, its role in this organ remains to be explained [8,9]. ADM stimulates cyclic guanosine monophosphate (cGMP) production via nitric oxide (NO) in various cell types [10,11], and cGMP inhibits meiotic resumption [12,13], thereby maintaining oocytes at the GV stage [14]. On the basis of these findings, we speculated that ADM might be a novel regulator of meiotic resumption. In the present study, we found that ADM can prevent spontaneous oocyte GVBD and meiotic resumption in the presence of an NO donor.

2. Materials and methods

2.1. Animals

This study was conducted in accordance with the Guide for the Care and Use of Laboratory Animals published by Tohoku University. Imprinting control region (ICR) mice were purchased from Japan SLC, Inc. (Shizuoka, Japan). Immature 20- to 23-day-old ICR mice were used for all experiments.

* Corresponding author. Fax: +81 22 717 8687.
E-mail address: hiradate@bios.tohoku.ac.jp (Y. Hiradate).

0006-291X/$ - see front matter © 2011 Elsevier Inc. All rights reserved.
doi:10.1016/j.bbrc.2011.10.139

2.2. Oocyte isolation and culture

To stimulate follicle development, each mouse was injected with 5 IU of pregnant mare's serum gonadotropin (PMSG) (Teikoku Hormone MGF, Tokyo, Japan). Cumulus–oocyte complexes (COCs) were collected 48 h after PMSG injection from large antral follicles punctured with 26-gauge needles in Leibovitz's L-15 medium (Invitrogen, Grand Island, USA) containing 0.1% polyvinyl alcohol (Sigma, St. Louis, MO). To prevent spontaneous meiotic resumption during COC collection, 300 μM dibutyryl cyclic adenosine monophosphate (dbcAMP; Sigma) was added to the medium. After washing in dbcAMP-free medium, the COCs were cultured in Waymouth's MB 752/1 medium (Invitrogen) supplemented with 5% fetal calf serum (Sankyo Kagaku, Kyoto, Japan), 0.23 mM pyruvic acid (Nacalai Tesque, Kyoto, Japan), 75 mg/L penicillin G (Meiji Seika, Tokyo, Japan), and 50 mg/L streptomycin sulfate (Meiji Seika). Approximately 20 COCs were cultured in 100-μL droplets of culture medium overlaid with paraffin liquid (Nacalai Tesque) in a humidified atmosphere of 5% CO_2 in air at 37 °C.

2.3. Chemical treatments

A 100× stock solution of ADM (Phoenix Pharmaceuticals, Burlingame, CA) and sodium nitroprusside (SNP; Sigma) was prepared in culture medium. SH-6 (Calbiochem, La Jolla, CA), U0126 (Cell Signaling Technology, Danvers, MA) and PP2 (Calbiochem) were dissolved in dimethyl sulfoxide (DMSO; Sigma). The working stocks were further diluted in culture medium to the final desired concentration in each experiment.

2.4. Assessment of GVBD occurrence

At the end of culture, cumulus cells from the COCs were removed by glass needle pipetting and scored using microscopy for the occurrence of GVBD. The percentage of oocytes at the GV stage was obtained by dividing the number of oocytes at the GV stage by the total number of cultured oocytes.

2.5. Reverse transcription polymerase chain reaction (RT-PCR)

Total RNA extraction from cumulus cells and oocytes was performed using an RNeasy Micro kit (Qiagen, Hilden, Germany) following the manufacturer's instructions. For cumulus cell and oocyte RNA extraction, approximately 100 COCs were denuded by repeated pipetting with a glass needle until the all the oocytes in the medium were aspirated. After the oocytes were separated, the cumulus cell-containing medium was transferred to 1.5-mL tubes and gently centrifuged. The cumulus cells were then obtained from the pellet. Total RNA was stored at −80 °C until use. Total RNA was reverse transcribed with SuperScript II (Invitrogen) using poly $(dT)^{12-18}$ primers (Invitrogen). The cDNAs were amplified using primers and Taq DNA polymerase (Takara Bio, Tokyo, Japan). The primer sequences of *crlr* (Genbank ID:018782), *ramp1* (Genbank ID:146522), *ramp2* (Genbank ID:019444), *ramp3* (Genbank ID:019511), and *gapdh* (Genbank ID:008084) are listed in Table 1. The PCR conditions for each treatment were as follows: denaturation at 94 °C for 5 min, 35 cycles of denaturation at 94 °C for 45 s, annealing at random temperatures (as listed in Table 1) for 45 s, extension at 72 °C for 45 s, and final extension at 72 °C for 5 min. The amplified PCR products were separated on a 2% agarose gel by electrophoresis and stained with ethidium bromide.

2.6. Immunoblotting

Protein from cumulus cells was collected from approximately 80–100 COCs cultured with 1, 10, and 100 nM of ADM for 6 h. Extraction was performed using sodium dodecyl sulfate (SDS) sample buffer, 0.5 M Tris–HCl (pH 6.8), 10% 2-mercaptoethanol, and 20% glycerol, and the proteins were separated by 12% SDS–polyacrylamide gel electrophoresis (SDS–PAGE) and transferred onto a membrane for 90 min. The membranes were immersed for 60 min in blocking solution 5% w/v skim milk for or 5% w/v bovine serum albumin (BSA) and incubated overnight at 4 °C in Tris-buffered saline and Tween 20. The antibodies used for detection were as follows: goat polyclonal anti-Akt (diluted 1:2000; Cell Signaling Technology), goat polyclonal anti-serine phosphorylated Akt (diluted 1:1000; Cell Signaling Technology) or mouse anti-α-tubulin monoclonal (diluted 1:2000; Sigma). After the incubation, the membranes were washed 3 times and incubated with horseradish peroxidase-conjugated goat anti-rabbit IgG or goat anti-mouse IgG (diluted 1:20,000; Jackson ImmunoResearch, PA) for 1 h at room temperature. The chemiluminescence was visualized using an ECL Plus system (GE Healthcare Ltd., UK).

2.7. Immunohistochemistry

Immunohistochemical analysis was performed to elucidate the localization of ADM. Ovaries were collected from 3 weeks mice. The samples were fixed in 4% formalin solution for 2 days and embedded in paraffin. The samples were divided into 5-μm-thick slices, deparaffinized, and rehydrated. After blocking the nonspecific protein binding by 5% BSA, sections were treated with rabbit anti-ADM antibody (diluted 1:500; Santa Cruz Biotechnology) overnight at 4 °C. The sections were next treated with Alexa Fluor 488-labeled goat anti-rabbit immunoglobulin antibody (diluted 1:1000; Santa Cruz) and counterstained with propidium iodide (100 μg/mL). Images of the sections were acquired using a Zeiss LSM700 confocal microscope.

2.8. Statistical analysis

Statistical differences between the means of the 2 groups were analyzed by Student's *t*-test. For the analysis of >2 groups, we used analysis of variance followed by a Bonferroni/Dunn test with STATVIEW (Abacus Concepts Inc., Berkeley, CA). Data are represented as mean ± SD and means were considered different when $P < 0.05$.

3. Results and discussion

3.1. mRNA expression of ADM receptor in cumulus cells and oocytes

Several factors are reported to have an inhibitory effect on GVBD. For example, hypoxanthine isolated from porcine follicular fluid prevents spontaneous oocyte maturation [15]. In addition, reactive oxygen species such as nitric oxide can affect oocyte maturation [16]. However, the precise mechanism of oocyte maturation has not been completely elucidated, and it is likely that other regulators have yet to be identified. This study aimed to determine whether ADM might be one such regulator.

We first investigated the expression of ADM receptor mRNA in cumulus cells and oocytes. As mentioned in the introduction, *crlr* must be co-expressed with *ramp2* or *ramp3* to create a functional ADM receptor. As shown in Fig. 1, *crlr* and *ramp1*, *ramp2*, and *ramp3* mRNAs were detected in cumulus cells but not in oocytes, suggesting that a functional ADM receptor is selectively expressed in cumulus cells. Numerous studies have indicated that cumulus cells

Table 1
Primers used in RT-PCR.

Gene	Primer sequences (5′–3′)	Product size (bp)	Annealing (°C)
crlr	Forward: TGG CTT TTC CCA CTC TGA T Reverse: TCA CAT CAC TAG ATC ATA CGT	157	53
ramp1	Forward: GAC GCT ATG GTG TGA CT Reverse: GAG TGC AGT CAT GAG CAG	249	55
ramp2	Forward: CAT GGA CTC TGT CAA GGA CTG Reverse: GTG TAT CAG GTG AGC CT	153	55
ramp3	Forward: ACC TGT CGG AGT TAC TCG Reverse: ATC AGT GTG CTT GCT GCT	262	58
gapdh	Forward: CCACTCTTCCACCTTCGATG Reverse: GAGGGAGATGCTCAGTGTTG	226	55

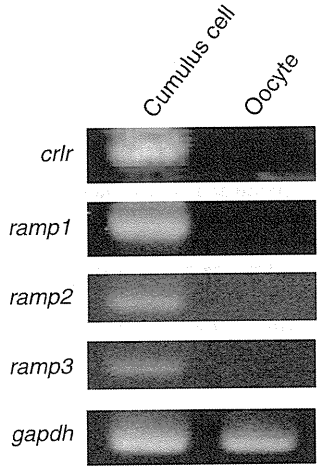

Fig. 1. mRNA expression of the ADM receptor. Reverse transcriptase polymerase chain reaction (PCR) was performed as described in Section 2 in mouse cumulus cells (A) and oocytes (B). The mRNAs of *crlr*, *ramp1*, *ramp2*, and *ramp3* were detected only in the cumulus cells and not in the oocytes. The resultant PCR products were separated on a 2% agarose gel and stained with ethidium bromide.

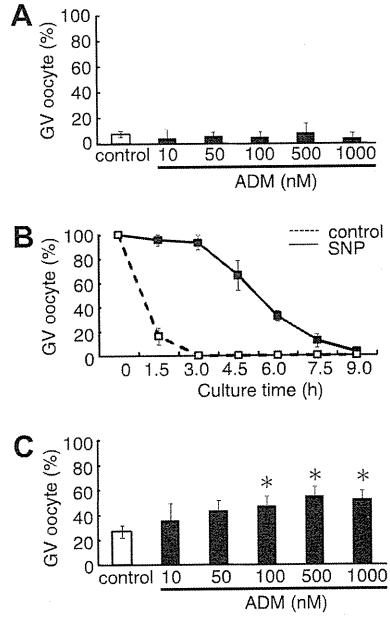

Fig. 2. Effect of ADM on germinal vesicle (GV) breakdown prevention. Cumulus–oocyte complexes (COCs) were cultured in the maturation medium with (10–1000 nM) or without ADM for 6 h (A). Time-course profiling of the percentage of oocytes at the GV stage when 1 mM of sodium nitroprusside (SNP) was added to the culture medium for 9 h (B). COCs were cultured in medium with (10–1000 nM) or without ADM containing 1 mM of SNP for 6 h (C). Values of the mean ± SD were calculated for 3 independent experiments. Data were analyzed using *t*-test. $^{*}P < 0.05$.

are important upstream regulators of GVBD since they are a source of cGMP, which maintains oocytes in meiotic arrest [13,17]. The movement of cGMP from cumulus cells to oocytes is facilitated by gap junctions formed by the tight association of these cells. This flow is present until gap junctions are closed due to luteinizing hormone activity [18].

3.2. Effect of ADM on GVBD prevention

We next examined whether ADM treatment could prevent GVBD. The addition of ADM to COCs did not influence GVBD at any concentration; in fact, no significant difference was found at 10–1000 nM (Fig. 2A). However, it is possible that, in our culture model, we lacked factors that normally co-operate with ADM to block GVBD *in vivo*. Pre-ovulatory follicles in rats contain a high-concentration milieu of nitric oxide (NO) [19]. NO produced by the nitrogen donor SNP leads to increased cGMP production by stimulating NO-dependent guanylyl cyclase activity [20]. Furthermore, cGMP production can be stimulated by ADM in various cell types [21–23]. Since cGMP is a crucial factor that controls GVBD, NO is thought to be one of the oocyte maturation inhibitors. We hypothesized that ADM works synergistically with NO to elevate cGMP levels. We therefore examined whether other known stimulators of cGMP production might cooperate with ADM in this manner.

In oocyte *in vitro* maturation, Bu et al. reported that SNP treatment induced meiotic arrest in mouse oocytes [24]. Consistent with this finding, the addition of 1 mM SNP prevented almost all oocyte GVBD 1.5 and 3 h after the start of culture and then gradually decreased (Fig. 2B). We then chose the 6-h time point to evaluate the synergistic effect of ADM in the presence of SNP because it was difficult to distinguish the effect of ADM from that of SNP in the condition in which almost all oocyte GVBD was prevented. We observed that in the presence of SNP, ADM significantly prevented oocyte GVBD at 100, 500, and 1000 nM since the frequency of oocytes at the GV stage was 47.23 ± 7.84%, 55.22 ± 7.18%, and 52.06 ± 7.47%, respectively, compared to that of control (27.05 ± 5.07%) (Fig. 2C). Taken together, these results suggest that ADM requires SNP-derived NO to inhibit GVBD. When COCs were cultured with ADM and 8-Br-cGMP, a cGMP analog, GVBD prevention was not observed (data not shown). These results imply that the additional effects of NO but not of cGMP are required for ADM to function as a meiotic inhibitor.

3.3. Effects of Akt, mitogen-activated protein kinase (MAPK), and focal adhesion kinase (FAK) inhibitor

The above results suggest that ADM can induce GVBD prevention in the presence of elevated NO and cGMP levels. Adrenomedullin exerts it effects through activation of the Akt, MAPK, and FAK signaling pathways [25]. Therefore, we examined the effects of the inhibitors of these kinases on the inhibition of GVBD by ADM. When 20 μM of Akt inhibitor SH-6 [26,27] was added in the presence of ADM, the fraction of oocytes at the GV stage was 33.96 ± 7.85%, which was significantly lower than that obtained with treatment by ADM only (56.78 ± 10.34%). This result is supported by a report that showed that induction of cGMP following